

REVIEW ARTICLE

Discovery of Novel GABAAR Allosteric Modulators Through Reinforcement Learning

Amit Michaeli¹, Immanuel Lerner^{1,*}, Maria Zatsepin¹, Shaul Mezan¹ and Alexandra Vardi Kilshtain¹¹Pepticom Ltd, Jerusalem, Israel

Abstract: Background: As not all target proteins can be easily screened *in vitro*, advanced virtual screening is becoming critical.

Objective: In this study, we demonstrate the application of reinforcement learning guided virtual screening for γ -aminobutyric acid A receptor (GABAAR) modulating peptides.

Method: Structure-based virtual screening was performed on a receptor homology model. Screened molecules deemed to be novel were synthesized and analyzed using patch-clamp analysis.

Results: 13 molecules were synthesized and 11 showed positive allosteric modulation, with two showing 50% activation at the low micromolar range.

Conclusion: Reinforcement learning guided virtual screening is a viable method for the discovery of novel molecules that modulate a difficult to screen transmembrane receptor.

ARTICLE HISTORY

Received: June 05, 2020
Accepted: August 16, 2020

DOI:

10.2174/138161282666201113104150

Keywords: Virtual Screening, structure-based drug design, peptides, chlorine channel, allosteric, *in silico*, reinforcement learning.

1. INTRODUCTION

Traditional discovery efforts for novel ligands are centered around physical screening methodologies that were optimized to keep costs at reasonable levels. Techniques such as high throughput screening robots [1] emerged for small molecules, along with biological display technologies for biomolecules such as peptides; initiated by the Nobel prize winning phage display libraries [2, 3], followed by second generation display technologies have introduced the inclusion of non-natural amino acids [4] and macrocycles [5] into expressed systems. The common feature of all screening systems is a need to physically synthesize and screen large numbers of molecules to identify “hits”, so that despite the emergence of breakthrough methodologies, costs remain substantial. High costs often limit screening to validated drug targets and keeping screening technologies out of the reach of many researchers, perhaps delaying the emergence of new validated targets.

The introduction of virtual, *in-silico* screening methods can potentially reduce costs substantially. These methodologies have been classified into ligand-based approaches that typically define a common pharmacophore of existing known ligands and structure-based approaches that typically “dock” candidate molecules into the 3D target structure [6]. Structure-based approaches are independent of existing ligands, allowing the discovery of novel ligands. Structure-based approaches are enabled by the ever-growing Protein Data Bank [7], which makes a wide range of protein structure solutions publicly available. This was exemplified by the SARS-CoV-2 epidemic, in which the structure solutions of many novel viral targets were deposited within months of the initial onset.

GABA is the main inhibitory neurotransmitter in both vertebrate and invertebrate organisms [8]. GABA receptors are divided into two major classes, the GABA_A ionotropic chlorine (Cl⁻) channels and the G protein-coupled GABA_B receptors. GABA_A receptors

play a crucial role in the central nervous system (CNS) in homeostasis and pathological conditions, such as anxiety disorder, epilepsy, insomnia, spasticity, aggressive behavior, and other pathophysiological conditions and diseases [9]. The wide range of associated processes and conditions make GABA_A receptors attractive drug targets. As transmembrane ion channels, GABA_A channels enable physical high throughput screening for complicated molecules, inspiring the development of novel reporter cell lines for efficient screening [10]. Even with efficient reporter-gene cell lines, physical molecular screening remains challenging, making virtual screening methods attractive.

In this study, we report the application of reinforcement learning directed virtual peptide screening for novel GABA_A channel modulators. Reinforcement learning is a field of machine learning that tackles problems using agents that learn behavior through trial and error, receiving rewards for favorable actions [11]. This methodology differs from supervised learning in that a large training dataset is not required, allowing the discovery of truly novel molecules. This methodology has been previously applied for the discovery of a novel Y329S Glycogen Branching Enzyme chaperone [12] and novel, bispecific MD2/CD14 activating peptides [13]. As no known peptide GABA_A channel modulators are known, ligand-based approaches were less applicable, making it an ideal reinforcement learning test-case. In this study, we used reinforcement learning virtual screening on a homology model of the receptor, selected novel peptides for synthesis and characterized their activity using patch-clamp analysis.

2. MATERIALS AND METHODS

2.1. Target Structure Preparation

A 3D structure of the target protein is required as input for reinforcement learning of optimized, structure-based searches. Since no specific human $\alpha 1\beta 3\gamma 2$ structure was available, the human Type-A γ -aminobutyric acid receptors (GABAAR) in the $\beta 3$ -homo-trimer composition (PDB: 4COF) [14] were downloaded from the Protein Data Bank [7]. The human $\alpha 1\beta 3\gamma 2$ sequence (supplementary data) was then threaded on to the backbone, followed by the addition of hydrogens and minimization using the

*Address correspondence to this author at the Pepticom Ltd, Jerusalem, Israel; Tel/Fax: ++972-54-481-9947, +972-50-640-70161; E-mail: Immanuel.lerner@pepticom.com

Schrödinger software Prime suit (Schrödinger Release 2017-1: Prime, Schrödinger, 2017) (20, 21). A subsequent structure of the human $\alpha 1\beta 3\gamma 2$ structure was deposited in the PDB: 6153 [15] and concurred well with our model (RMSD<1Å). Structure comparisons and visualization were performed using the PyMOL Molecular Graphics System, Version 1.8; Schrödinger (New York, NY).

2.2. Peptide Discovery

Structure-based peptide discovery was performed using the LINEPEP module that uses reinforcement learning algorithms based on risk-return heuristics as previously described [16]. In brief, potential docking decisions are analyzed using both risk and return parameters. Return is assessed as the potential binding-energy contribution of a particular decision, whereas risk is assessed as a measure of the sum of returns of all mutually exclusive decisions. Potential decisions are then eliminated if found inefficient, exposing more risk than decisions of similar returns. When applied in reinforcement learning, each decision can be analyzed as having both an expected risk and an expected return, with the exploration probability taking both factors into account.

To focus on the discovery of peptides that bind with the GABA binding site, a 15Å search grid was centered around tyrosine 62 of chain E of the threaded structure model. Side chain composition was limited to the 20 natural amino acids for the initial screening, with non-natural subunits used after the initial screening to validate the binding model.

2.3. Peptide Synthesis

Lyophilized peptides were produced at EMC Microcollections (Tubingen, Germany) and stored at 20°C until use. Peptides were reconstituted/dissolved in DMSO as concentration of either 10 mM or otherwise to the highest possible concentration as indicated. Sonication was used to dissolve the peptides if necessary. For each experiment, the stock solution was diluted in DMEM to the appropriate working concentration (between 1 mM and 0.1 mM). The peptides are diluted in such a way that the final DMSO concentration in minimal media did not exceed 0.1%.

2.4. Activity Analysis

GABAAR activity was analyzed by manual whole-cell patch-clamp technique at B'SYS GmbH (Witterswil, Switzerland) on $\alpha 1\beta 3\gamma 2$ GABAAR Transfected HEK293 cells, measuring chlorine currents upon introduction of GABA and/or tested peptides.

Recombinant HEK293 cells were continuously maintained in and passaged in sterile culture flasks containing a 1:1 mixture of Dulbecco's modified eagle medium and nutrient mixture F-12 (DMEM/F-12 1x, liquid with L-Glutamine supplemented with 10% fetal bovine serum and 1.0% Penicillin/Streptomycin solution, supplemented with the following selection antibiotics: 300 µg/mL Geneticin, 100 µg/mL Hygromycin B and 25 µg/mL Zeocin.

In general, cells were passaged at a confluence of about 50%-80%. For electrophysiological measurements cells were harvested from sterile culture flasks, containing culture complete medium and plated on Poly-L-Lysine coated coverslips. Confluent clusters of cells are electrically coupled. Because responses in distant cells are not adequately voltage-clamped, and because of uncertainties regarding the extent of coupling, cells were cultivated at a density that enables single cells (without visible connections to other cells) to be measured.

As an initial calibration, GABA inward currents were measured upon application of submaximal GABA concentration (2 µM) to patch-clamped cells. The cells were voltage-clamped at a holding potential of -80 mV. If current density was judged to be too low for measurement, another cell was recorded. To test for peptide agonist activity, 30 seconds after the last GABA application, 100 µM of the tested peptides were perfused without GABA. This

was followed by a test for antagonist/modulator activity; after 5 seconds of pre-incubation of test item, GABA receptors were stimulated by GABA (2µM) in the presence of the same test item concentration. Finally, following washing of the cells, 100 µM Pentobarbital was used as a positive control.

2.5. EC₅₀ Determination

SigmaPlot 11.0 was used to construct the dose-response curves with a sigmoidal three-parameter equation:

$$\text{Current (peak, relative)} = \frac{E_{\max}}{1 + 10^{(\log [EC_{50} - X])H}}$$

Where, X is the drug concentration, E_{max} the upper asymptote, EC₅₀ the concentration of the test item at half-maximal effect, and H is the Hill coefficient.

3. RESULTS

As no human $\alpha 1\beta 3\gamma 2$ GABAAR structure was available at the time of the initiation of this study, a modelled structure was used as input and retroactively shown to be of high fidelity (RMSD<1Å); for clarity sake, the residue numbers and chains reported herein will be the ones used in the solved structure (PDB: 6153) [15]. The peptide search grid was located in the interface formed by the $\beta 3$ and $\alpha 1$ subunits.

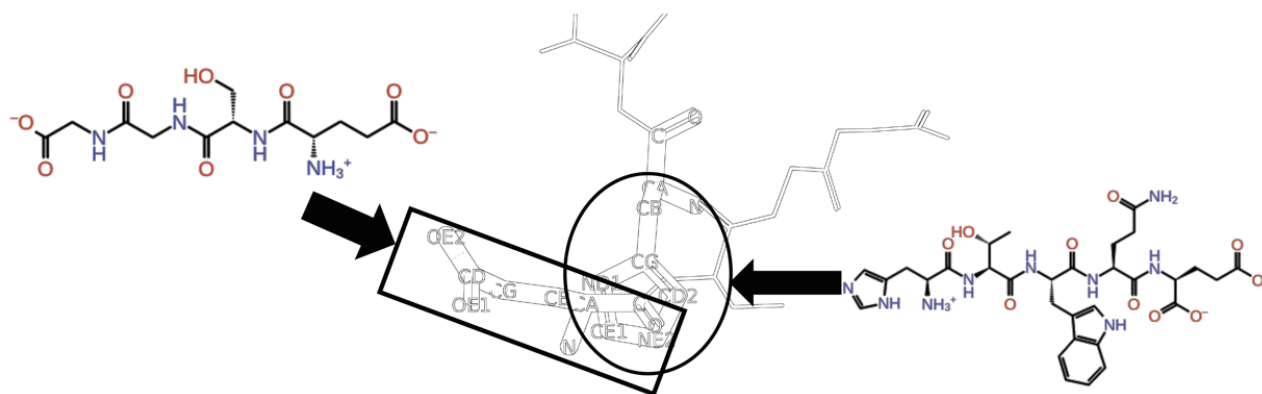
The peptide solution set was clustered into two primary backbone models: Peptides centered around an N-terminal glutamic acid and peptides centered around an N-methyl histidine, with arginine outliers (Fig. 1A). Additionally, a few of the cluster peptides were selected: RFHS, KTTSI and TESKG-CONH₂.

The N-terminal glutamic acid group showed a calculated binding energy contribution distribution that was heavily leaning towards the N-terminal glutamic acid, which in itself can be considered a GABA analogue with three aliphatic carbons connecting the NH₃⁺ motif to the COO⁻ motif. To further illustrate this, we superimposed our model GABAAR to a rat $\alpha 1\beta 1\gamma 2$ S solved structure (PDB: 6DW0)[17] with a calculated RMSD of 1.1Å. The N-terminus glutamic acid was indeed positioned very similarly to the GABA, with a distance of 0.7Å between the COOH- carbon groups, with 2.2Å between the NH₃⁺ nitrogen atoms (Fig. 1B). Additionally, the GABA-like cluster was significantly smaller (4 unique members) than the N-methyl histidine group (10 members) (Fig. 1C). We hence ruled out this group for lacking novelty, and it was not further analyzed.

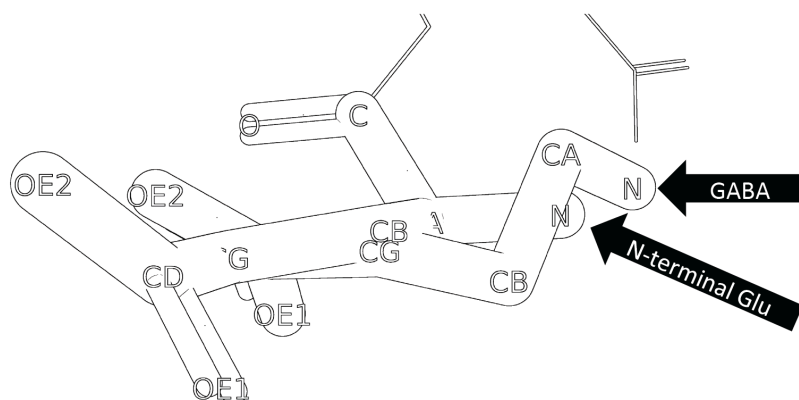
The N-methyl histidine group was synthesized and tested using the patch-clamp technique on $\alpha 1\beta 3\gamma 2$ GABAAR transfected HEK293 cells for initial screening. Cellular chlorine currents were measured at the base level with GABA alone and the peptides alone, and with the peptides together with GABA. As a positive control, 500mM of Pentobarbital was used together with 2µM GABA.

None of the peptides showed agonist activity, and no significant chlorine current change was observed when peptides were introduced alone. When the peptides were introduced with GABA, significant potentiation was measured when compared to GABA alone. This pattern was shared by all members of the N-methyl Histidine cluster, suggestive of a common mode of action. The 8 peptides of the cluster ranged in increased potentiation from 40% to 380%, when measured at peptide concentrations of 100µM (Table 1).

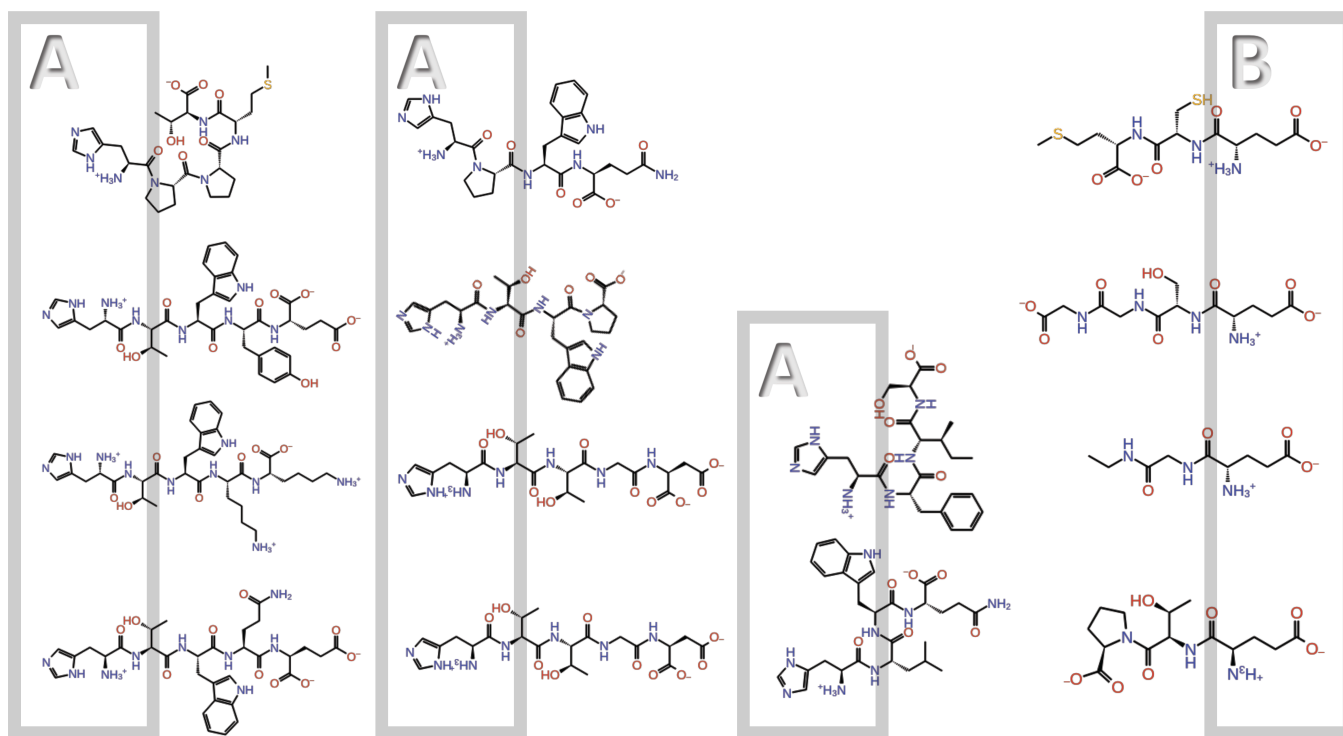
The two most potent peptides were selected for dose-response analysis. The HTWQE peptide showed maximal potentiation (E_{max}) of 388% (Supplementary Fig. 1) with a dose-response reaching 50% excitation (EC₅₀) at 6.5µM (Hill coefficient = 1.24) (Fig. 2A). The Q4Y variant HTWYE showed an E_{max} of 285%, (Supplementary Fig. 7) with an EC₅₀ of 3.7µM (Hill coefficient = 1.01) (Fig. 2B).



A) The solution peptides were clustered into two main clusters by backbone Root Means Squared Deviation. One cluster was dominated by N-term histidine residues (circle) and the other by N-terminal glutamic acid residues.



B) Superimposition of the glutamic acid cluster to a solved receptor structure with GABA (PDB: 6DW0) revealed a high degree of similarity between the modeled glutamic acid and GABA.



C) The members of the two main reinforcement learning solution set clusters A: share the histidine N-term binding mode and B. share a glutamic acid binding mode.

Fig. (1). Solution set clusters. (A higher resolution/colour version of this figure is available in the electronic copy of the article).

Table 1. N-term histidine cluster, GABAAR allosteric activation.

S. No.	Position:	1	2	3	4	5	% Increased Excitation	Supplementary Figure:
1	-	H	T	W	Q	E	388	1
2	-	H	T	W	K	K	41	6
3	-	H	T	W	Y	E	280	7
4	-	H	P	P	A	T	92	8
5	-	H	I	S-CONH2			61	9
6	-	H	T	T	G	D	211	12
7	-	H	T	W	P		169	14
8	-	H	P	W	Q		124	15
9	-	R	T	W	Q	E	n.d.	
10	-	R	T	W	G	E	53	13

Peptides were clustered by backbone root means square deviation (RMSD). The most dominant cluster was dominated by N-terminal histidine residues (8/10). The peptides were synthesized and their activity was analyzed by patch-clamp analysis on GABAAR expressing HEK293 cells. Complete experimental data is available at the referenced supplementary figure.

The N-terminal histidine that defined the cluster was also predicted by the software to be the dominant binding energy contributor, binding deep in the GABAAR pocket, an area with an abundance of aromatic rings. This could allow histidine to have a significant binding energy contribution, regardless of its modeled hydrogen bonds. To validate this, we synthesized two hydrophobic variants of HTWQE, modeled to be spatially compatible with its binding model: (2-fluoro-L-phenylalanine)TWQE and (L-cyclohexylalanine)TWQE; both peptides showed the same allosteric activator activity pattern as HTWQE (224% and 62%, at 100 μ M, respectively) (Supplementary Figs. 5 and 2).

The N-terminal histidine residue was also modeled to potentially interact electrostatically with the backbone oxygen of α 1 tyrosine 160, serving as a hydrogen bond donor. One of the cluster's outliers, RTWGE showed a similar backbone conformation as HTWQE (RMSD<0.1Å) and showed moderate allosteric activation, increasing chlorine ion flow by 53% at 100 μ M (Supplementary Fig. 13). The replacement of histidine with arginine was also modeled to additionally serve as a hydrogen bond donor to the α 1's threonine 207 and tyrosine 210 sidechains.

The N-terminal backbone nitrogen, normally cationic in biologic solutions, was modeled to form a salt-bridge with β 3's aspartate in position 43, coupled by a cation- π interaction with β 3's tyrosine 62.

Position 2 was dominated by threonine, predicted to bind the threonine in position 176 of the β 3 subunit, with a possible additional interaction with asparagine 41 of the same subunit. As the backbone nitrogen atom was predicted to be buried without an electrostatic interaction, some of the models replaced threonine with proline (Table 1), trading favorable electrostatic interactions with more favorable desolvation. In both cases, the position 2 backbone oxygen was modeled to receive hydrogen bonds from serine 206 side-chain and backbone nitrogen of α 1.

Position 3 was dominated by tryptophan, contributing to binding primarily by hydrophobic interactions. Similar interactions were modeled with proline. Threonine and serine in position 3 were modeled to donate a hydrogen bond to the backbone of position 204 of chain α 1.

Position 4 was modeled to interact with the backbone oxygen of β 3 lysine in position 173 when composed of lysine, tyrosine or glutamine. Other variants of position 4 included alanine, glycine

and proline, indicating that binding energy rewards for this position are not dominant.

When glutamic or aspartic acid were modeled in position 5, the primary contribution was a salt bridge with the β 3 lysine in position 173. This salt bridge is modeled to be primarily solvated, providing a modest calculated binding energy contribution. This was, however, found experimentally to exist in the 3 most potent peptides.

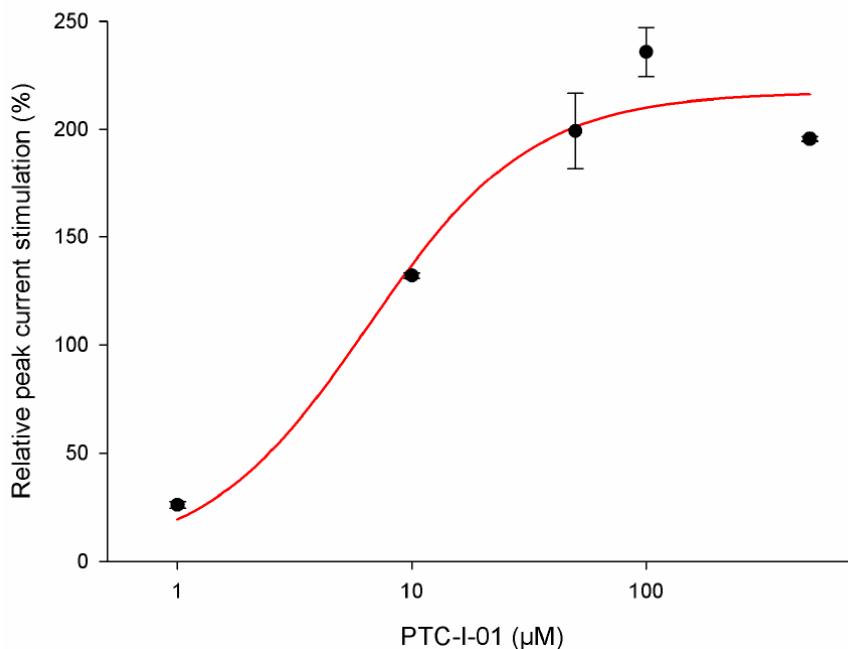
Our model suggested that the HTWQE binding model can be compatible with methylation of histidine side chain and threonine/tryptophan backbones. The (3-methyl-L-histidine) (N-methyl-threonine) (N-methyl-tryptophan)QE peptide was synthesized and showed increased potentiation of 106%, when measured at peptide concentrations of 100 μ M (Supplementary Fig. 4). A similar peptide, without the tryptophan methylation, has shown increased potentiation of 58% at 100 μ M (Supplementary Fig. 3).

The non-clustered peptide models were also screened at 100 μ M. The RFHS and TESKG-CONH2 peptides showed allosteric potentiation increases of 91% and 46%, respectively (Supplementary Figs. 10 and 11). The KTTSI peptide showed no significant effect on chlorine ion flow when introduced alone or with GABA.

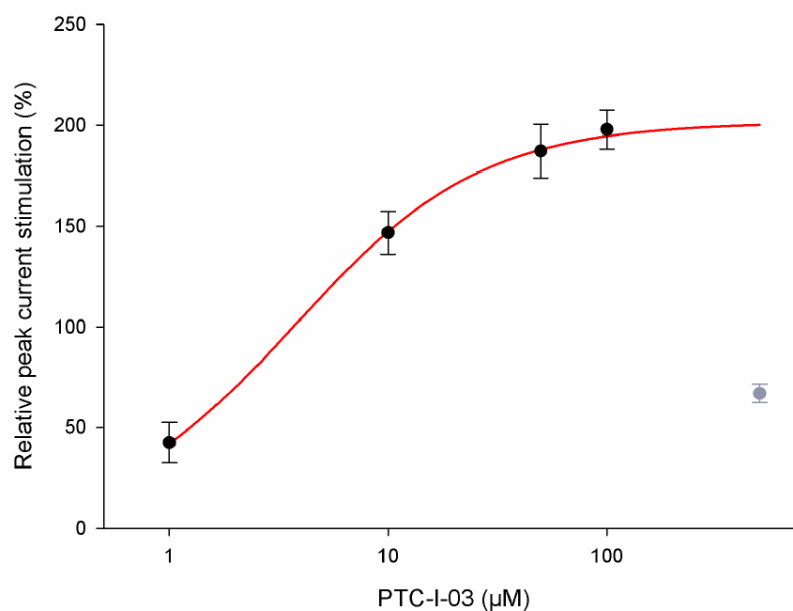
4. DISCUSSION

In this study, we used reinforcement learning guided virtual screening to discover novel peptide modulators for α 1 β 3 γ 2 GABAAR. Large chemical spaces, coupled with rather lengthy docking procedures, currently limit exhaustive virtual screening efforts. Reinforcement learning provides a potentially unbiased approach, avoiding training sets of supervised learning, which naturally carry a bias towards molecules that mimic known ligands.

The basic heuristic of reinforcement learning involves the creation of agents or "bots" that perform the docking task. Each "bot" is composed of sequence selection, docking and learning algorithms that enable it to dock peptides to the target protein. As the process evolves, "bots" exchange information and methodologies between them, allowing for more efficient sequence selection and docking processes. The underline goal of this strategy is to create a process which increases the speed and scope of virtual screening while least compromising the quality of the calculated solution set.



A) HTWQE (PTC-I-01) modulated the response to GABA (2μM) in a dose-dependent manner. The EC_{50} value was determined to 6.50 μM (Hill coeff. 1.24). E_{max} was determined to 217.19%.



B) HTWYE(PTC-I-03) modulated GABA (2μM) response in a dose-dependent manner. The EC_{50} value was determined to 3.72 μM (Hill coeff. 1.01). E_{max} was determined to 201.50%. Results at 500 mM were not used for EC_{50} determination.

Fig. (2). Patch-clamp dose-response of GABAAR transfected HEK293 cells. (A higher resolution/colour version of this figure is available in the electronic copy of the article).

One of the critical dilemmas faced by a “bot” is whether to better exploit its current solution, or alternately, explore the conformational and grid spaces. So, for example, if a bot is tasked at docking a sequence such as ATQRS, it may exploit the already docked model of a sequence such as ASQRS, threading the query sequence to it, or explore a novel solution by docking ATQRS without this prior knowledge. The management of this dilemma is one of the key challenges in molecular screening by reinforcement learning. Over exploring will render the method too slow, essen-

tially turning it into a virtual screening method while over exploiting may miss out on novel solutions. Alternately, once a significant number of sequences have been docked, efficiently exploiting the solved solution set becomes a tedious task as well, with the side chain exploit search space being equal to (number of subunit types)^(chain length) threaded sequences per each docked backbone model.

We have previously reported that heuristics taken from financial portfolio management can be deployed to manage the exploit

process more efficiently [16]. In this Risk Adjusted Design (RAD) method, “bots” calculate a structural “risk” and “return” values for each possible mutation in each position; the bots then exploit the docked backbones threading the individual positions of each docked structure only with side chains included in the “risk/return efficient set”, dramatically minimizing the exploitation search space [16]. This threading can later serve new “bots” to further dock additional sequences based on the threaded sequences, so using the sequence from the above example, a new bot that selected the ATQRSW sequence can exploit the docked sequences of ATQRS or other similar sequences using “bot” defined preferences, exploring only possible locations for W or docking the entire sequence.

In this case, reinforcement learning provided two solution clusters for the relatively small pocket formed by the $\beta 3$ and $\alpha 1$ subunits: A GABA-like cluster, which could have been theoretically provided by GABA pharmacophore-based screening (Fig. 1A and 1B) and the histidine cluster (Fig. 1A). The GABA-like cluster was smaller in both the number of solutions and the number of amino-acids per each solution (Fig. 1C). This highly suggested that reinforcement learning converged on to a GABA centered consensus sequence, and in fact, attempted to re-create GABA using the amino-acid building blocks available to it. This is impressive at the machine learning level, as the software was unaware that the input target structure was a GABA receptor, nor did the input included a reference structure of GABA. However, for practicality, the GABA-like cluster lacked novelty, as it could have been derived theoretically from the pharmacophore of GABA. The histidine cluster, which showed no similarity to any known ligands, was selected for synthesis and testing for the discovery of new, novel ligands.

The molecules of this cluster showed positive allosteric modulator activity. This phenomenon is more consistent with the previously reported benzodiazepines (BZD) positive allosteric modulators [18].

The benzodiazepine diazepam (DZP, Valium) recently had been analyzed using HEK293 patch-clamp analysis showing an EC_{50} of 7.428nM with an efficacy of 171.9% for GABA [19]. The structure of diazepam bound to the $\alpha 1\beta 3\gamma 2$ GABAAR has been solved (PDB: 6HUP)[20]. Diazepam was shown to bind the $\alpha 1/\gamma 2$ pocket and upon superimposition to our $\alpha 1/\beta 3$ - HTWQE model (RMSD<1Å), it showed an aromatic ring located in the same area as our histidine side chain. A similar observation was also repeated in the solved structure of GABAAR with alprazolam (ALP, Xanax) (PDB: 6HUO)[20]. The backbone oxygen of residue 1 showed proximity (<1Å) to the oxygen of diazepam.

Superimposition of our peptide binding $\alpha 1/\beta 3$ pocket models to diazepam’s $\alpha 1/\gamma 2$ pocket showed plausible compatibility. The aromatic rings that characterized the model of histidine 1 were preserved, as were the $\alpha 1$ interactions modeled for arginine in position 1. The N-terminal backbone nitrogen showed cation- π interaction with $\gamma 2$ ’s tyrosine 58 and phenylalanine 77. In position 2, the backbone oxygen retained the hydrogen bond donations from $\alpha 1$. The side chain of position 2 did not seem to form significant interactions. The residues of position 3 retained their $\alpha 1$ binding model, whereas positions 4 and 5 remained primarily solvated and did not form specific interactions with the receptor. This relatively high binding mode compatibility suggests that the peptides bind either the $\alpha 1/\beta 3$ pocket, the $\alpha 1/\gamma 2$ pocket or both. Further investigation is required to clarify the exact mode of action.

CONCLUSION

In this study, we used reinforcement learning guided virtual screening to discover novel GABAAR modulating peptides. Two peptides with EC_{50} values in the low micromolar range were discovered out of 13 peptides screened. This demonstrates a good

feasibility study for the virtual screening option for targets that are difficult to screen *in vitro*, such as membrane ion channels.

ETHICS APPROVAL AND CONSENT TO PARTICIPATE

Not applicable.

HUMAN AND ANIMAL RIGHTS

No Animals/Humans were used for studies that are base of this research.

CONSENT FOR PUBLICATION

Not applicable.

AVAILABILITY OF DATA AND MATERIALS

Not applicable.

FUNDING

None.

CONFLICT OF INTEREST

The authors declare no conflict of interest, financial or otherwise.

ACKNOWLEDGEMENTS

Declared none.

SUPPLEMENTARY MATERIAL

Supplementary material is available on the publisher’s website along with the published article.

REFERENCES

- Macarron R, Banks MN, Bojanic D, *et al.* Impact of high-throughput screening in biomedical research. *Nat Rev Drug Discov* 2011; 10(3): 188-95. <http://dx.doi.org/10.1038/nrd3368> PMID: 21358738
- Smith GP. Filamentous fusion phage: novel expression vectors that display cloned antigens on the virion surface. *Science* 1985; 228(4705): 1315-7. <http://dx.doi.org/10.1126/science.4001944> PMID: 4001944
- Smith GP, Petrenko VA. Phage Display. *Chem Rev* 1997; 97(2): 391-410. <http://dx.doi.org/10.1021/cr960065d> PMID: 11848876
- Hirose H, Tsiamantas C, Katoh T, Suga H. *In vitro* expression of genetically encoded non-standard peptides consisting of exotic amino acid building blocks. *Curr Opin Biotechnol* 2019; 58: 28-36. <http://dx.doi.org/10.1016/j.copbio.2018.10.012> PMID: 30453154
- Passioura T, Suga H. A RAPID way to discover nonstandard macrocyclic peptide modulators of drug targets. *Chem Commun (Camb)* 2017; 53(12): 1931-40. <http://dx.doi.org/10.1039/C6CC06951G> PMID: 28091672
- Pinzi L, Rastelli G. Molecular docking: Shifting paradigms in drug discovery. *Int J Mol Sci* 2019; 20(18): 4331. <http://dx.doi.org/10.3390/ijms20184331> PMID: 31487867
- Berman HM, Westbrook J, Feng Z, *et al.* The Protein Data Bank. *Nucleic Acids Res* 2000; 28(1): 235-42. <http://dx.doi.org/10.1093/nar/28.1.235> PMID: 10592235
- Gou ZH, Wang X, Wang W. Evolution of neurotransmitter gamma-aminobutyric acid, glutamate and their receptors. *Dongwuxue Yanjiu* 2012; 33(E5-6): E75-81. PMID: 23266985
- Jembrek MJ, Vlaimic J. GABA Receptors: Pharmacological Potential and Pitfalls. *Curr Pharm Des* 2015; 21(34): 4943-59. <http://dx.doi.org/10.2174/1381612821666150914121624> PMID: 26365137
- Kuenzel K, Friedrich O, Gilbert DF. A recombinant human pluripotent stem cell line stably expressing halide-sensitive YFP-I152L for GABAAR and GlyR-targeted high-throughput drug screening and toxicity testing. *Front Mol Neurosci* 2016; 9: 51. <http://dx.doi.org/10.3389/fnmol.2016.00051> PMID: 27445687

- [11] Kaelbling LP, Littman ML, Moore AW. Reinforcement learning: A survey. *J Artif Intell Res* 1996; 4: 237-85.
<http://dx.doi.org/10.1613/jair.301>
- [12] Froese DS, Michaeli A, McCorvie TJ, *et al.* Structural basis of glycogen branching enzyme deficiency and pharmacologic rescue by rational peptide design. *Hum Mol Genet* 2015; 24(20): 5667-76.
<http://dx.doi.org/10.1093/hmg/ddv280> PMID: 26199317
- [13] Michaeli A, Mezan S, Kühbacher A, *et al.* Computationally Designed Bispecific MD2/CD14 Binding Peptides Show TLR4 Agonist Activity. *J Immunol* 2018; 201(11): 3383-91.
<http://dx.doi.org/10.4049/jimmunol.1800380> PMID: 30348734
- [14] Miller PS, Aricescu AR. Crystal structure of a human GABAA receptor. *Nature* 2014; 512(7514): 270-5.
<http://dx.doi.org/10.1038/nature13293> PMID: 24909990
- [15] Laverty D, Desai R, Uchański T, *et al.* Cryo-EM structure of the human $\alpha 1\beta 3\gamma 2$ GABA_A receptor in a lipid bilayer. *Nature* 2019; 565(7740): 516-20.
<http://dx.doi.org/10.1038/s41586-018-0833-4> PMID: 30602789
- [16] Lerner I, Goldblum A, Rayan A, Vardi A, Michaeli A. From finance to molecular modeling algorithms: The risk and return heuristic. *Curr Top Pept Protein Res* 2017; 18: 117-31.
- [17] Phulera S, Zhu H, Yu J, Claxton DP, Yoder N, Yoshioka C, *et al.* Cryo-EM structure of the benzodiazepine-sensitive $\alpha 1\beta 1\gamma 2S$ trimeric GABAA receptor in complex with GABA. *Elife* [Internet] 2018. <https://elifesciences.org/articles/39383>
- [18] Squires RF, Brastrup C. Benzodiazepine receptors in rat brain. *Nature* 1977; 266(5604): 732-4.
<http://dx.doi.org/10.1038/266732a0> PMID: 876354
- [19] Witkin JM, Cerne R, Wakulchik M, *et al.* Further evaluation of the potential anxiolytic activity of imidazo[1,5-a][1,4]diazepin agents selective for $\alpha 2/3$ -containing GABA_A receptors. *Pharmacol Biochem Behav* 2017; 157: 35-40.
<http://dx.doi.org/10.1016/j.pbb.2017.04.009> PMID: 28442369
- [20] Masiulis S, Desai R, Uchański T, *et al.* GABA_A receptor signalling mechanisms revealed by structural pharmacology. *Nature* 2019; 565(7740): 454-9.
<http://dx.doi.org/10.1038/s41586-018-0832-5> PMID: 30602790

DISCLAIMER: The above article has been published in Epub (ahead of print) on the basis of the materials provided by the author. The Editorial Department reserves the right to make minor modifications for further improvement of the manuscript.